

Improving Colorectal Cancer Screening and Risk Assessment through Predictive Modeling on Medical Images and Records

Shuai Jiang, Ph.D.¹; Christina Robinson, M.S.^{2,3}; Joseph Anderson, M.D.^{4,5}; William Hisey, M.Sc.^{2,3}; Lynn Butterly, M.D.^{2,3,4}; Arief Suriawinata, M.D.⁶; *Saeed Hassanpour, Ph.D.*^{1,7,8,*}

Conflict of interest statement: Authors declare no conflict of interests.

Acknowledgement: This research was supported in part by grants from the US National Library of Medicine (R01LM012837 and R01LM013833) and the US National Cancer Institute (R01CA249758).

¹ Department of Biomedical Data Science, Geisel School of Medicine at Dartmouth, Hanover, New Hampshire

² Department of Gastroenterology and Hepatology, Dartmouth-Hitchcock Medical Center, Lebanon, New Hampshire

³ New Hampshire Colonoscopy Registry, Lebanon, New Hampshire

⁴ Department of Medicine, Dartmouth-Hitchcock Medical Center, Lebanon, New Hampshire

⁵ White River Junction VA Medical Center, Hartford, Vermont

⁶ Department of Pathology and Laboratory Medicine, Dartmouth-Hitchcock Medical Center, Lebanon, New Hampshire

⁷ Department of Epidemiology of Geisel School of Medicine at Dartmouth, Hanover, New Hampshire

⁸ Department of Computer Science, Dartmouth College, Hanover, New Hampshire

* *Correspondence: Saeed Hassanpour, PhD*

1 Medical Center Drive, HB 7261, Lebanon, NH 03756
Saeed.Hassanpour@dartmouth.edu

Abstract

Background and aims: Colonoscopy screening is an effective method to find and remove colon polyps before they can develop into colorectal cancer (CRC). Current follow-up recommendations, as outlined by the U.S. Multi-Society Task Force for individuals found to have polyps, primarily rely on histopathological characteristics, neglecting other significant CRC risk factors. Moreover, the considerable variability in colorectal polyp characterization among pathologists poses challenges in effective colonoscopy follow-up or surveillance. The evolution of digital pathology and recent advancements in deep learning provide a unique opportunity to investigate the added benefits of including the additional medical record information and automatic processing of pathology slides using computer vision techniques in the calculation of future CRC risk.

Methods: Leveraging the New Hampshire Colonoscopy Registry’s extensive dataset, many with longitudinal colonoscopy follow-up information, we adapted our recently developed transformer-based model for histopathology image analysis in 5-year CRC risk prediction. Additionally, we investigated various multimodal fusion techniques, combining medical record information with deep learning derived risk estimates.

Results: Our findings reveal that training a transformer model to predict intermediate clinical variables contributes to enhancing 5-year CRC risk prediction performance, with an AUC of 0.630 comparing to direct prediction (AUC = 0.615, $p = 0.013$). Furthermore, the fusion of imaging and non-imaging features, while not requiring manual inspection of microscopy images, demonstrates improved predictive capabilities (AUC = 0.674) for 5-year CRC risk comparing to variables extracted from colonoscopy procedure and microscopy findings (AUC = 0.655, $p = 0.001$).

Conclusion: This study signifies the potential of integrating diverse data sources and advanced computational techniques in transforming the accuracy and effectiveness of future CRC risk assessments.

Keywords: Colorectal cancer; cancer screening; vision transformer; multi-modal fusion

1 Introduction

It is estimated that 52,550 lives were lost in 2023 due to colorectal cancer (CRC) in the U.S., giving CRC the highest cancer mortality rate after lung cancer. Overall, 4.3% (1 in 23) of men and 3.9% (1 in 26) of women will be diagnosed with CRC in their lifetime¹. However, colorectal cancer can be *prevented* through regular screening procedures^{2,3}, since almost all CRC arises from colorectal polyps [thereafter, “polyp(s)”]⁴. Meanwhile, nearly half of Western adults will have a polyp in their lifetime, and one-tenth of these cases will progress to cancer⁵. Fortunately, it usually takes several years for these polyps to progress, leaving a window for removal and CRC prevention.

Currently in the U.S. it is recommended that all average-risk adults undergo CRC screening by the age of 45, while patients at increased risk, such as those with a family history of CRC in a close relative, need to start screening earlier. Colonoscopy screening is associated with a 40-67% reduction in the risk of death from colorectal cancer^{6,7}.

There are multiple “direct- visualization” screening methods to detect polyps, such as colonoscopy, sigmoidoscopy, and virtual colonoscopy. Among those, colonoscopy has become the most common screening test in the U.S.⁸. More than 15 million colonoscopies are performed in the U.S. each year^{9,10}. In 2021, it was estimated that 63.1% of US adults were up to date with colonoscopy screening, and it is expected the CRC screening will increase to cover 74.4% of Americans aged 50 to 75 years by 2030⁸.

In 2020, the U.S. Multi-Society Task Force on CRC issued updated guidelines on CRC surveillance after colonoscopy screening and polypectomy¹¹⁻¹³. The Task Force recognizes a range of CRC risk classifications for patients undergoing colonoscopies. The timing of the recommended follow-up colonoscopy depends on these categories: <5 years for high-risk, and 5-10 years for low-risk patients. Of note, according to the Task Force guidelines, risk and follow-up recommendations for patients undergoing colonoscopy depend only upon histopathological characterization (i.e., type), number, size, and location of polyps detected in previous colonoscopies. Therefore, the current screening and surveillance guidelines are limited and do not take into account many other CRC risk factors, such as age, race, body mass index, smoking/alcohol use, activity level, diet, and family history¹⁴⁻²³. Incorporating these relevant factors in colorectal cancer risk assessment aims to capture a comprehensive context to provide patients with a more accurate and efficient surveillance plan.

Another gap in CRC risk stratification arises from the microscopic examination of polyps. Although the recommended intervals between surveillance procedures depend on histopathological analysis¹², accurate reading can be a challenging task⁴ – currently, there is a significant amount of variability among pathologists in how they characterize and diagnose colorectal polyps²⁴⁻³⁵. For instance, sessile serrated polyps, which can develop dysplasia and progress to CRC are difficult to differentiate histologically from hyperplastic polyps³⁶⁻³⁸. The accurate characterization and differentiation of polyps can help patients to receive appropriate follow-up surveillance and to reduce unnecessary additional screenings, healthcare costs, and stress.

With the recent expansion of whole-slide digital scanning, high-throughput tissue banks, and archiving of digitized histological studies, the field of digital pathology is primed to benefit significantly from deep-learning models. A major advantage of deep learning for histopathological image analysis is eliminating the need to design application-specific, handcrafted features for training the model, thus can be applied to various tasks, including nucleus detection³⁹⁻⁴¹, tumor classification⁴²⁻⁴⁹, and patient outcome prediction⁵⁰⁻⁵³. As transformer models reshape the landscape of medical image analysis, they have been applied to CRC-related tasks, such as CRC segmentation⁵⁴ and colorectal polyp classification⁵⁵. In a substantial multi-center study, transformer models were observed to outperform CNN-based methods in predicting microsatellite instability⁵⁶.

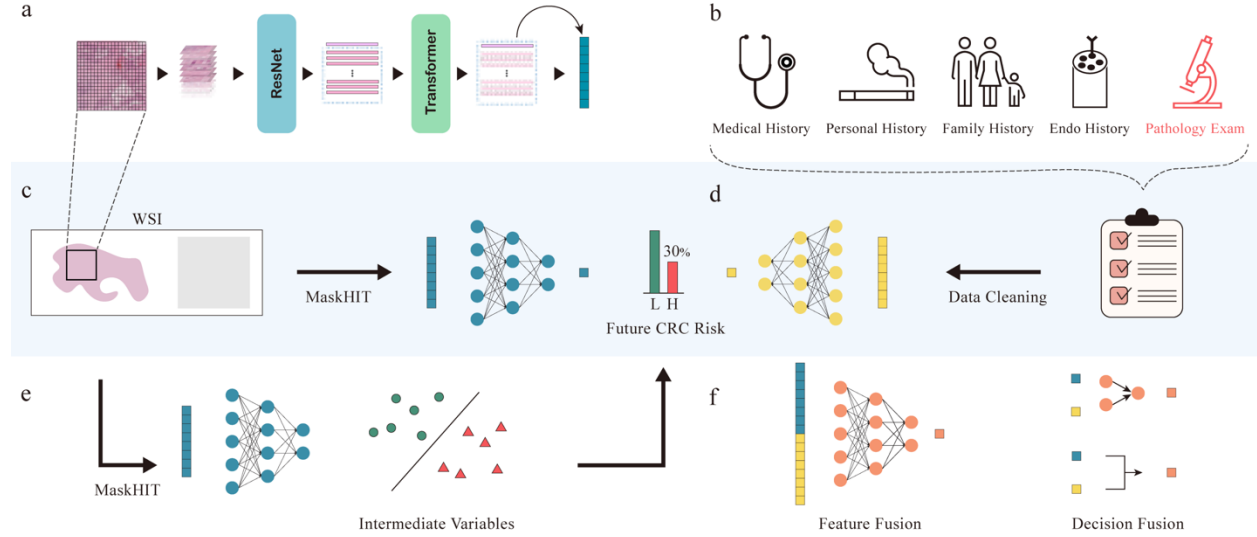
Histopathological information provides crucial insights into tumor characteristics; however, for a comprehensive analysis, the inclusion of non-image features is imperative. Multi-modal fusion is a key strategy for combining information from diverse modalities to augment prediction accuracy. These fusion techniques are broadly categorized into early fusion and late fusion. Early fusion involves concatenating features from each modality and training a unified model, while late fusion entails training individual models and combining their

decisions⁵⁷. Numerous studies adopt the approach of concatenating features from different modalities to construct a unified patient representation⁵⁸⁻⁶². Although feature-level fusion has the potential to capture intricate correlations among features, its flexibility may elevate the risk of overfitting. Conversely, some studies have demonstrated that simpler decision-level fusion techniques outperform feature-level fusion in certain scenarios^{63,64}.

A key requirement for developing accurate deep-learning methods is the access to large datasets for model training. Despite the rapid advancements in deep-learning technology and computational capabilities, there have not been major efforts to curate large, open access, and high-quality, annotated images for polyp analysis. The lack of “big data” in this domain makes it virtually impossible for existing or new deep-learning architectures to be developed for polyp histopathological characterization. In this study, we will utilize the data collected from New Hampshire (NH) Colonoscopy Registry (NHCR) for model development and evaluation.

The overall objective of this study is to develop and evaluate a novel, accurate, and automatic deep-learning method to analyze clinicopathological findings associated with colorectal polyps for colorectal cancer prevention by leveraging both imaging and medical record information. In a previous study⁶⁷, we developed a transformer-based pre-training and fine-tuning pipeline, MaskHIT, for medical image analysis. In this study, we adapt the MaskHIT model for automatic, accurate, and interpretable polyp characterization on histology images. In addition, we explored different fine-tuning strategies (direct vs. guided) and various multi-modal fusion techniques to improve CRC risk assessment based on both imaging and non-imaging data. We anticipate the improved accuracy in future CRC risk prediction would benefit colonoscopy participants in making more informed follow-up decisions.

Figure 1. Technical Overview. a) Illustration of the MaskHIT pipeline. b) Data sources of medical records. c) Direct prediction of 5-year CRC risk using WSI. d) Prediction of 5-year CRC risk using medical records. e) Guided attention approach that fine-tunes MaskHIT first for intermediate variables, then for the 5-year CRC risk. f) Different fusion methods.



2 Materials and Methods

2.1 Study population

The NHCR is an NCI-funded, statewide registry that contains comprehensive longitudinal colonoscopy information from nearly all endoscopy sites in NH since 2004. It includes patient risk factors, such as age; sex; personal and family history of polyps or CRC; weight; height; smoking status; alcohol consumption; endoscopy history; polyp sizes, locations, numbers, and treatment; pathology reports; follow-up recommendations; and follow-up outcomes^{65,66}. These data are extracted through a rigorous data collection effort from 31 participating practices, in addition to questionnaire responses from patients. The NHCR's collected data are unique in the U.S., in terms of its detailed, population-based, longitudinal and complete data. Dartmouth Hitchcock Medical Center (DHMC), a tertiary academic medical center in Lebanon, NH, has been participating in NHCR from its start in 2004 and, among patients who have their information recorded in the NHCR, over 30,000 of them are DHMC patients. The histology slides of these DHMC patients are stored at the Department of Pathology and Laboratory Medicine (DPLM) at DHMC and are available for this study.

The sources of data in this project include NHCR^{68,69} and pathology slides from DHMC. 5,159 patients who underwent colonoscopy at DHMC from 2004 to 2018 without a CRC diagnosis at index visit and have their CRC status reassessed in 5 years were included in this study. After excluding 2,561 patients without WSIs, and an additional 205 patients with missing clinical data, 2,393 patients were included in the training and evaluation of our proposed models. This dataset encompasses hematoxylin and eosin (H&E) stained WSIs with various types of polyps and normal cases, and patients' clinical records from NHCR.

2.2 Outcome

The NHCR and DHMC follow-up medical records are used to identify high-risk of CRC and to build the CRC risk reference standard labels for patients. Based on polyp recurrence rate, CRC progression time, and the recommended frequency for follow-up colonoscopies^{11,12}, in this study, we consider patients who developed CRC, advanced adenomatous polyps, or serrated polyps with dysplasia in the 5 years after screening as high-risk, while patients without those developments in 5 years following their baseline colonoscopies as low-risk. Advanced adenomatous polyps include polyps ≥ 1 cm, with villous components (TVA/V), or with high-grade dysplasia⁷⁰. Advanced adenomas and serrated polyps ≥ 1 cm or with dysplasia are known as surrogates for CRC and are widely used as high CRC risk indicators⁷¹⁻⁷⁵. The 5-year risk window is chosen to maximize the clinical utility, based on our use case in this project and the current guidelines for follow-up colonoscopy rate^{11,12}.

2.3 Clinical features and image data

Under the review and approval of the Committee for the Protection of Human Subjects, we extracted the following information from the NHCR database: 1) Identifiers of patients with tissue removed during colonoscopy, including the pathology Case-ID, used to locate tissue slides and access WSIs; 2) types, numbers, and sizes of polyps identified in the baseline colonoscopy exam; 3) microscopic determination of the tissue type of the polyps; and 4) relevant medical information for patients from the NHCR relational database.

The medical information was collected from NHCR Procedure Forms, completed by endoscopists or endoscopy nurses at participating sites and patient questionnaire responses. The NHCR database covers a comprehensive list of CRC risk factors based on peer-reviewed publications^{65,66}. The variables we extracted from the NHCR database are summarized in four categories, as shown in Supplementary Table 1.

H&E-stained WSIs, scanned at DHMC (Aperio AT2, Leica Biosystems), were processed using MaskHIT pipeline. Briefly, color thresholding technique was used to create tissue masks. Non-overlapping patches of size $224\mu\text{m} \times 224\mu\text{m}$ (i.e., 448×448 pixels) on $20 \times$ ($0.5\mu\text{m}/\text{pixel}$) magnification level were extracted, along with their positions on the WSI.

2.4 Risk prediction using WSIs

The MaskHIT architecture is employed for predicting 5-year CRC risk using WSIs. MaskHIT can effectively model the relative positional information of patches on a large region from WSI. In the pre-training phase, Masked AutoEncoder (MAE) technique was used, by first randomly masking out a portion of patches from the sampled region, then using the output from the transformer model to restore the feature representations of those masked locations. This process helps the model capture relationships between different patches and their histopathologic features and understand the context. The original MaskHIT model was pretrained using more than 10 cancer types from the Cancer Genome Atlas (TCGA) database. The MaskHIT model achieved improved performance in cancer survival prediction and cancer subtype classification tasks compared to state-of-the-art models.

The workflow of the MaskHIT model involves the extraction of square regions, comprising up to 400 patches, from WSIs. Subsequently, a ResNet model, pre-trained on ImageNet data⁷⁶, is utilized for feature extraction. The location information of the patches, along with the extracted features, is then fed into a transformer model, which comprises 8 attention heads and 12 attention layers. The output of the transformer model yields a class token, serving as a representation of the entire region. Multiple regions can be sampled from a single WSI concurrently, and the class tokens are averaged to generate a global summarization of the WSI. This global summarization is then employed for risk classification through a linear projection layer (Figure 1a, Figure 1c).

To tailor the MaskHIT model pre-trained on TCGA to the specific context of polyp analysis, we conducted an additional pre-training phase for 200 epochs, employing the same pre-training methodology as previously described⁷⁷.

During the fine-tuning stage, we randomly sampled 4 non-overlapping regions from each patient. Each region comprised up to 400 patches, each of size 448×448 pixels at a magnification level of $20\times$. To mitigate computational costs, 25% of patches were randomly sampled from each region. During the evaluation phase, a maximum of 64 regions were sampled from each patient across all slides that this patient has, to estimate their respective CRC risk.

3 Beyond the direct risk prediction using WSIs, an alternative training approach, named "guided prediction" (Figure 1

e), was explored. In this procedure, a MaskHIT model was initially fine-tuned to predict intermediate variables derived from patients' medical records or microscopic examinations of polyps. Subsequently, this model was employed to predict patients' future CRC risk. Two strategies were compared: 1) freezing the weights of the transformer model and exclusively fine-tuning the last linear projection layer for outcome prediction; 2) fine-tuning both the transformer model weights and the last linear projection layer. The guided prediction approach only utilizes intermediate variables during the training procedure to assist the MaskHIT model in focusing on more relevant regions in the WSIs.

3.1 Combination of clinical and image histopathological information

The non-imaging variables underwent preprocessing, where continuous variables were standardized, and categorical variables were one-hot encoded, resulting in a feature vector of dimension 69. Missing values were imputed by replacing them with either the average value for continuous variables or the most common class for categorical variables.

Common approaches for risk prediction, such as penalized logistic regression, multi-layer perceptron network (MLP), and random forest (RF), were explored for modeling non-imaging variables. Each approach was evaluated through cross-validation on a small subset withheld from the training data to select the optimal architecture for modeling non-imaging variables.

We excluded microscopy exam findings from building the final fusion model given the forementioned burden and variability related to obtaining such information from colonoscopy exams. Various strategies for integrating non-imaging variables with WSI features were investigated, including feature-level aggregation and decision-level aggregation (Figure 1f). Feature-level aggregation, belonging to the early fusion technique, involved concatenating non-imaging features with those extracted from the transformer output of WSIs. Subsequently, patient outcomes were predicted using multiple layers of linear projections. In decision-level fusion, predicted risk probabilities from non-imaging and WSIs were combined either through averaging or by assigning different weights to each component.

3.2 Evaluation

In this study, 25% of our dataset (i.e., slides and records for 600 patients) was held out as the test set for the evaluation of the developed methods, and the remaining 75% was used as the training set. A five-fold cross-validation was conducted on the training dataset for hyperparameter tuning. We use the area under the curve (AUC) of receiver operating characteristic (ROC) to assess the model's performance. To ensure a more robust estimate of model performance, the train/test splitting process was repeated 10 times, and the average performance along with the standard deviation (std) on the test splits was reported. Paired t-tests across repeated experiments were utilized to calculate the statistical significance ($p < 0.05$) of the compared methods.

3.3 Model interpretation and visualization

A significant limitation of current deep-learning methods is their black-box nature, where the focus is primarily on the efficacy of the final results, with little attention given to providing clear explanations or evidence of the factors that contribute to these outcomes. To address this issue and gain a deeper understanding of the pertinent regions on WSI influencing risk predictions, we computed the difference in attention scores between the pre-trained transformer model and the transformer model fine-tuned for outcome prediction. These attention score differences were then color-coded and overlaid onto the WSIs, enabling insights into the shift in model attention for each specific outcome prediction task.

For the multimodal fusion model that integrates non-imaging information with WSI, interpretability was enhanced by calculating Shapley values for both non-imaging features and WSI risk predictions. These Shapley values were aggregated across repeated experiments, and the average scores were plotted for visualization, providing a transparent depiction of the contributions of each feature to the model's predictions.

4 Results

4.1 Description of study population

A description of the demographical features of the study population is shown in Supplementary Table 2. Of 2,393 patients, 1,994 (83.3%) remained in the low-risk category after 5 years, while 399 (16.7%) developed high risk findings. The patients who developed high CRC risk in 5 years were significantly older than those remained in the low CRC risk category (62.0 vs. 58.7 years old, $p < 0.001$), and were more likely to be male (60.7% vs. 51.9%, $p = 0.002$). The majority of the study population are non-Hispanic Caucasian, and the distribution of race and ethnicity does not differ by risk group. The description of other groups of variables are available in the supplementary materials.

4.2 Risk prediction using WSIs

In the direct prediction of 5-year CRC risk using WSIs, the MaskHIT model attained an average AUC of 0.615. We evaluated multiple intermediate variables, including size and number of adenomas, size and number of serrated lesions, and all of them combined. Furthermore, the use of polyp tissue types obtained from microscopic examinations as intermediate variables was explored, including most advanced serrated lesion, and most advanced adenoma (**Error! Reference source not found.**).

MaskHIT demonstrates robust predictive performance for various intermediate variables, with notable AUC values. The highest AUC is achieved when predicting the most advanced serrated lesion (AUC: 0.927 ± 0.007), followed closely by predictions for the most advanced adenoma (AUC: 0.902 ± 0.004). The prediction of the number of adenomas found in colonoscopy yields a slightly lower AUC at 0.800 ± 0.007 . Overall, MaskHIT exhibits effective predictive capabilities across a range of intermediate variables.

These colonoscopy or microscopy findings can predict 5-year CRC risk with various performances (**Error! Reference source not found.**). Measurements of the size and number of adenomas were better at predicting 5-year CRC risk than measurements of serrated lesions. The best predictor among them was number of adenomas (AUC: 0.643 ± 0.029), while the AUCs obtained using measurements of serrated lesions were no better than random guess. Microscopy measurements, while still contributing to prediction, achieve an AUC of approximately 0.55 in forecasting 5-year CRC risk.

Upon employing the guided attention approach, where the MaskHIT model was initially fine-tuned for intermediate variables and subsequently fine-tuned for 5-year CRC risk prediction, most intermediate variables exhibited an enhancement in outcome prediction performance. The best performance was observed when utilizing the size of the largest known serrated lesion as the intermediate variable, achieving an AUC of 0.629 ± 0.016 , although this variable itself cannot predict 5-year CRC risk better than random guess. When incorporating all colonoscopy variables as intermediate variables, the MaskHIT model achieved an average AUC of $0.622 (\pm 0.015)$ when the transformer backend was frozen. Further fine-tuning the transformer backend for risk prediction resulted in an average AUC of $0.630 (\pm 0.016)$,

representing a statistically significant improvement compared to the direct prediction approach.

When variables from the microscopic exam of the polyps were used as the intermediate variables, "Most advanced serrated" polyp significantly improved the average AUC to 0.625 (± 0.018) with transformer fine-tuned, which was statistically better than the direct prediction approach. While for "most advanced adenoma", the differences in average AUC were not statistically significant.

Table 1. Comparison of direct prediction versus guided attention prediction using WSIs, AUC (std.)

Fine-tuning strategy	Intermediate variable	WSI \rightarrow intermediate	Intermediate \rightarrow Risk	WSI \rightarrow risk	
				Freeze Transformer	Fine-tune Transformer
Direct prediction	None	-	-	-	0.615 (0.016)
Guided by colonoscopy exam	Largest known adenoma size	0.889 (0.004)	0.593 (0.026)	0.625 (0.016)	0.626 (0.016)*
	Number of adenomas	0.800 (0.007)	0.643 (0.029)	0.624 (0.014)	0.625 (0.016)
	Largest known serrated	0.897 (0.004)	0.511 (0.034)	0.623 (0.018)	0.629 (0.016)*
	Number of serrated lesions	0.864 (0.002)	0.482 (0.037)	0.614 (0.028)	0.622 (0.014)
	All above variables	-	0.651 (0.027)	0.622 (0.015)	0.630 (0.016)*
Guided by microscopy exam	Most advanced serrated	0.927 (0.007)	0.546 (0.019)	0.625 (0.018)	0.625 (0.018)*
	Most advanced adenoma	0.902 (0.004)	0.550 (0.024)	0.618 (0.018)	0.620 (0.016)
* p-value < 0.05; P-values were calculated as comparing the guided prediction results to the direct prediction using paired t-test.					

4.3 Risk prediction using medical records

The performance comparison of L2 penalized logistic regression, random forest, and neural network (NN) models for predicting 5-year CRC risk using non-imaging variables is presented in **Error! Reference source not found..** Among these three prediction methods, no clear winner emerges. Variables extracted from colonoscopy exams demonstrated the best performance in predicting 5-year CRC risk (AUC: 0.653-0.658), followed by personal history-related variables (AUC: 0.589-0.594). Both medical history variables and endoscopy history variables showed the capability to predict 5-year AUC with an AUC of at least 0.54. However, family history variables did not seem to contribute significantly to CRC risk prediction. The combination of the two microscopy exam variables (most advanced serrated and most advanced adenoma) predicted 5-year CRC risk with an AUC between 0.54 and 0.55.

Table 2. Risk prediction using non-imaging variables, AUC (std.)

Category	L2-Logistic	Random Forest	NN
----------	-------------	---------------	----

Personal history	0.594 (0.030)	0.589 (0.024)	0.594 (0.029)
Medical history	0.543 (0.035)	0.526 (0.026)	0.541 (0.033)
Family history	0.510 (0.022)	0.519 (0.020)	0.509 (0.018)
Endoscopy history	0.536 (0.025)	0.549 (0.032)	0.546 (0.027)
Colonoscopy exam	0.657 (0.020)	0.653 (0.027)	0.658 (0.023)
Microscopy exam	0.550 (0.025)	0.543 (0.025)	0.545 (0.026)

4.4 Multi-modal prediction

Error! Reference source not found. compares different fusion strategies, including decision level average and weighting, and the incorporation of WSI predicted risk score and WSI extracted features with non-imaging features. The results were stratified by the strategy of fine-tuning the MaskHIT model for 5-year risk prediction. When the MaskHIT model was trained using the direct prediction approach, the best performance was achieved by using the weighted average of the independent probabilities from WSIs and the non-imaging information (AUC = 0.672 ± 0.020). With guided prediction training, the best performance was $0.675 (\pm 0.018)$ using average decision fusion. On average, the decision level fusion does not only provide improved performance, but also lower variation across the 10 repeated experiments compared to feature level fusion.

In **Error! Reference source not found.**, the 5-year CRC prediction performances resulting from diverse combinations of colonoscopy and microscopy findings, WSI risk predictions, and clinical variables are presented. In this experiment we used weighted decisions to fuse WSI-based predicted probabilities with the predicted probability from non-imaging features. Using only colonoscopy findings yielded an average AUC of $0.658 (\pm 0.023)$. The inclusion of microscopy findings demonstrated a marginal adverse impact on the predictive performance for 5-year CRC risk, resulting in an AUC of $0.655 (\pm 0.021)$. Incorporating WSI-predicted risk scores and additional clinical features led to noteworthy improvements, presenting average AUC values of $0.669 (\pm 0.018)$ and $0.669 (\pm 0.027)$, respectively. The combination of both aspects of information further increased the average AUC to $0.674 (\pm 0.021)$, marking a statistically significant improvement compared to utilizing colonoscopy findings alone ($p=0.004$) and the combination of colonoscopy and microscopy findings ($p=0.001$).

Table 3. Comparison of fusion techniques, AUC (std.)

Fusion Method	Direct	Guided
Decision average	0.670 (0.014)	0.675 (0.018)
Decision weighted	0.672 (0.020)	0.674 (0.021)
WSI decision + Non-imaging features	0.661 (0.031)	0.668 (0.022)
WSI features + Non-imaging features	0.664 (0.024)	0.668 (0.024)
Non-imaging features include colonoscopy findings and additional medical records. Boldface shows the best performance of each column.		

Table 4. Comparison of input modalities, performance (std.)

Input Modalities	AUC	Accuracy	F1	Precision	Recall
Colonoscopy	0.658 (0.023)	0.646 (0.025)	0.351 (0.031)	0.251 (0.021)	0.585 (0.068)
Colonoscopy+Microscopy	0.655 (0.021)	0.650 (0.021)	0.346 (0.023)	0.250 (0.015)	0.566 (0.061)
Colonoscopy+WSI	0.669 (0.018)	0.655 (0.019)	0.351 (0.026)	0.254 (0.017)	0.571 (0.066)
Colonoscopy+Clinical	0.669 (0.027)	0.645 (0.026)	0.359 (0.029)	0.255 (0.023)	0.604 (0.046)
Colonoscopy+WSI+Clinical	0.674 (0.021)	0.644 (0.021)	0.362 (0.027)	0.257 (0.019)	0.615 (0.059)
Boldface shows the best performance of each column.					

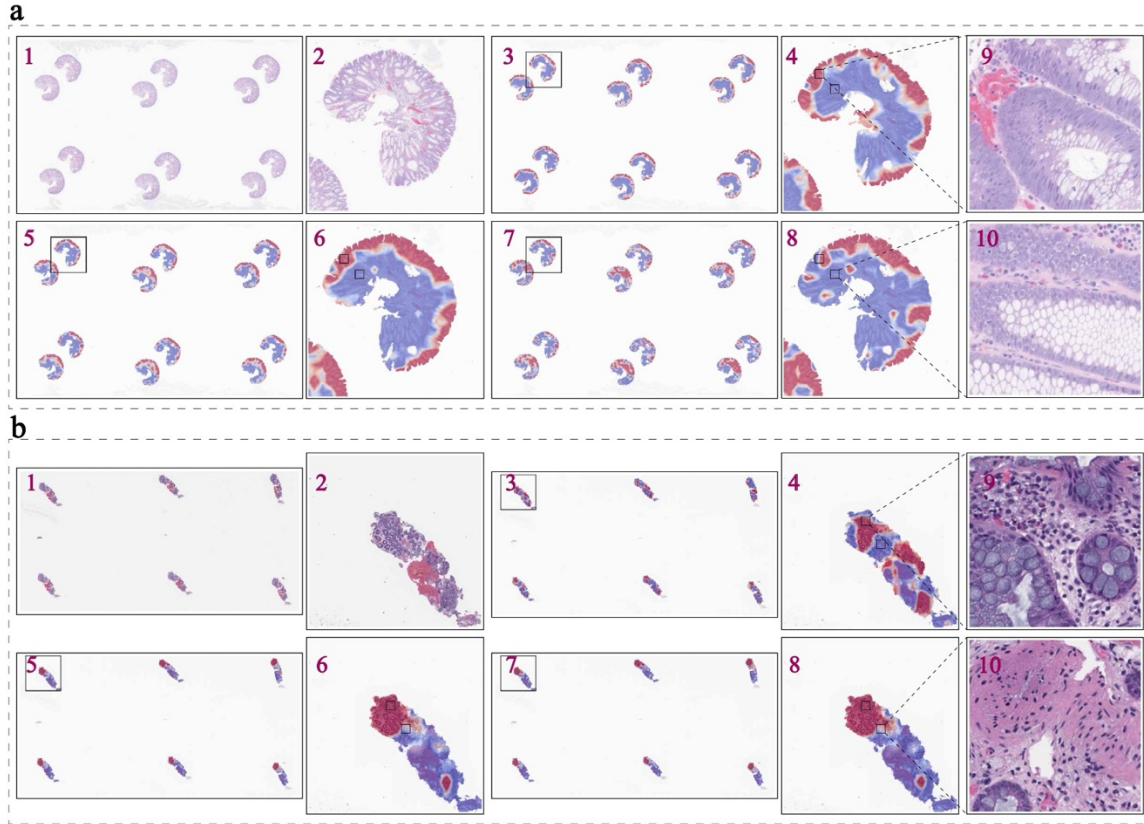
4.5 Model interpretation

4.5.1 Attention map visualization

The attention maps obtained from the MaskHIT model for two WSIs are presented in Figure 2a for a high-risk patient and Figure 2b for a low-risk patient. The visualization reveals that the MaskHIT model tends to focus more on the structures of polyps within the WSIs. Interestingly, the high attention areas appear similar whether guided fine-tuning methods were employed or not.

The intensity of attention weights from the direct prediction approach and the guided prediction approach was further examined by calculating the difference in attention weights between these two methods. The results are presented in panels 7 and 8 of Figure 2. The redder color in these panels indicates that the highlighted region received higher attention from the guided prediction model compared to the direct prediction model. This visualization demonstrates that the regions receiving higher attention from the guided prediction model generally align with the regions attended by both the direct prediction model and the guided prediction model. In essence, the guided prediction model exhibited greater confidence in assigning weights to regions that were deemed important for risk prediction.

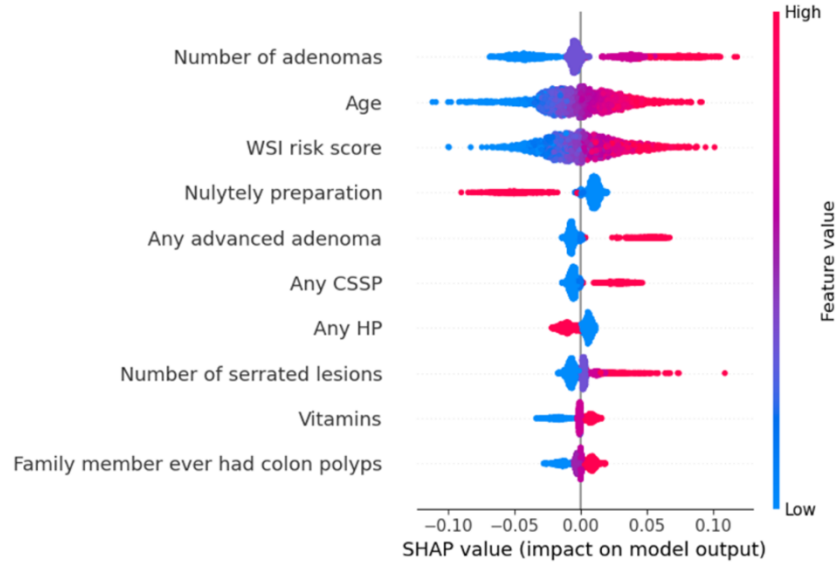
Figure 2. Attention maps for two WSIs. a) High risk patient; b) Low risk patient. Sub panels: 1&2: slide/region thumbnails; 3&4: attention map generated from direct prediction model; 5&6: attention map generated from guided attention model; 7&8: attention maps generated by taking the difference between guided attention map and direct attention map; 9&10: detailed patch view.



4.5.2 Feature importance ranking

In Figure 3, the top 10 most important features influencing the output of the final fusion model are presented. The most influential feature is the number of adenomas, demonstrating a positive association with 5-year CRC risk. Notably, the predicted risk probability from the WSI was ranked as the third most important feature in the fusion model, exceeded only by the number of adenomas and age.

Figure 3. *Shapley values of top 10 predictors in the fusion model (CSSP: Colorectal Sessile Serrated Polyp, HP: Hyperplastic Polyp)*



5 Discussion

The accurate prediction of future CRC risk is crucial for informed decisions regarding follow-up colonoscopy visits. Existing guidelines recommend leveraging polyp characteristics identified in colonoscopy exams, as well as some personal and family history risk factors, for patient risk stratification to determine the timing of subsequent colonoscopies¹¹. This study sought to advance future CRC risk prediction by integrating automatic deep learning-based analysis of whole-slide images and incorporating CRC-related medical information in a predictive multi-modal pipeline.

Relying exclusively on colonoscopy and microscopy aspects resulted in an average AUC of 0.655. However, by incorporating deep learning predicted probabilities and information from clinical variables, a statistically significant improvement in the prediction AUC to 0.674 was observed. This underscores the potential of leveraging advanced computational techniques and multimodal data fusion to enhance CRC risk assessment beyond conventional guidelines. Such an approach provides a more robust foundation for personalized and effective follow-up strategies in clinical practice.

To enhance the prediction performance utilizing WSIs, we refined our approach by adopting the recently developed model, MaskHIT. MaskHIT is a transformer-based method that leverages the location information of patches extracted from the entire slide. The unique aspect of the transformer model as a patch-level feature fusion technique lies in its capacity to incorporate spatial details, enabling our deep learning model to capture high-level structural information of the polyps. This approach stands in contrast to commonly used multiple instance learning approaches, offering a more nuanced and comprehensive representation of the intricate characteristics of colorectal polyps in our predictive model.

In addition, we conducted experiments involving a guided prediction approach to improve the transformer model for 5-year CRC risk prediction. As presented in **Error! Reference source not found.**, predicting 5-year CRC risk using WSI poses challenges due to numerous factors beyond current histopathological features from colonoscopy exams that can influence future CRC risk. Consequently, the MaskHIT model may face difficulties in confidently identifying visual features linked to CRC risk in this complex context.

To tackle this challenge, we adopted a guided prediction approach, enabling the transformer model to first predict histopathological features derived from the colonoscopy exam. Remarkably, MaskHIT demonstrated strong performance in this task, with AUCs exceeding 0.8 and considerably smaller standard deviations compared to risk prediction tasks. Subsequently, fine-tuning the MaskHIT model for risk prediction led to a statistically significant improvement compared to the direct prediction approach. Interestingly, certain variables, although ineffective at predicting future CRC risk independently, also contributed to enhancing MaskHIT’s accuracy in 5-year CRC risk prediction.

Attention map visualizations supported our hypothesis, revealing that the guided prediction model assigned greater attention weights to locations relevant for risk prediction (i.e., polyps) compared to the direct prediction model. This nuanced approach demonstrates the effectiveness of leveraging the guided prediction approach to enhance the interpretability and performance of deep learning models in the context of 5-year CRC risk prediction from whole-slide images.

We conducted further exploration of various approaches for combining information from colonoscopy exams, WSIs, and clinical records. In general, decision-level fusion produced superior results compared to models combining non-image features with risk predictions from the slides. Due to the high predictive value of colonoscopy variables, the signal from WSIs predictions can be easily overwhelmed by noise in clinical features, a known issue in multi-modal fusion⁷⁸. However, through the application of decision-level fusion techniques, this challenge can be addressed, resulting in improved outcomes compared to using either modality in isolation, consistent with findings in previous studies^{63,64}.

As the future steps, we plan to validate our multi-modal CRC risk approach using additional datasets. Furthermore, as our goal is to incorporate the additional information in the risk stratification for patients undergoing colonoscopy in the screening and surveillance program, we intend to quantify its health outcomes and cost impacts through follow-up clinical trials and prospective studies.

6 Conclusion

In this study, the integration of the transformer-predicted risk score and additional clinical information resulted in an improvement in the performance of CRC risk stratification. Notably, variables describing colonoscopy and microscopy findings of polyps were identified as contributors to enhanced performance in predicting 5-year CRC risk using deep learning models. Despite its simplicity in multi-modal fusion, decision-level fusion demonstrated superior performance improvements when combining imaging and non-imaging

information. Future research is essential to refine deep learning methods for including more related clinical information and to evaluate the additional benefits of an accurate CRC risk stratification in colonoscopy screening programs.

7 References

1. Siegel, R. L., Miller, K. D., Wagle, N. S. & Jemal, A. Cancer statistics, 2023. *CA A Cancer J Clinicians* **73**, 17–48 (2023).
2. Zauber, A. G. *et al.* Colonoscopic polypectomy and long-term prevention of colorectal-cancer deaths. *New England Journal of Medicine* **366**, 687–696 (2012).
3. Atkin, W. S. *et al.* Once-only flexible sigmoidoscopy screening in prevention of colorectal cancer: a multicentre randomised controlled trial. *The Lancet* **375**, 1624–1633 (2010).
4. Kumar, V., Abbas, A. K., Fausto, N. & Aster, J. C. *Robbins and Cotran Pathologic Basis of Disease*. (Elsevier Health Sciences, 2014).
5. Holt, P. R., Kozuch, P. & Mewar, S. Colon Cancer and the Elderly: From Screening to Treatment in Management of GI Disease in the Elderly. *Best practice & research. Clinical gastroenterology* **23**, 889 (2009).
6. Doubeni, C. A. *et al.* Effectiveness of screening colonoscopy in reducing the risk of death from right and left colon cancer: a large community-based study. *Gut* gutjnl-2016-312712 (2016) doi:10.1136/gutjnl-2016-312712.
7. Ma, W. *et al.* Association of Screening Lower Endoscopy With Colorectal Cancer Incidence and Mortality in Adults Older Than 75 Years. *JAMA Oncology* **7**, 985–992 (2021).
8. Sabatino, S. A. *et al.* Up-to-Date Breast, Cervical, and Colorectal Cancer Screening Test Use in the United States, 2021. *Preventing Chronic Disease* **20**, (2023).
9. Peery, A. F. *et al.* Burden of gastrointestinal disease in the United States: 2012 update. *Gastroenterology* **143**, 1179–1187 (2012).

10. Joseph, D. A. *et al.* Colorectal cancer screening: Estimated future colonoscopy need and current volume and capacity. *Cancer* **122**, 2479–86 (2016).
11. Lieberman, D. A. *et al.* Guidelines for colonoscopy surveillance after screening and polypectomy: a consensus update by the US Multi-Society Task Force on Colorectal Cancer. *Gastroenterology* **143**, 844–857 (2012).
12. Gupta, S. *et al.* Recommendations for follow-up after colonoscopy and polypectomy: a consensus update by the US Multi-Society Task Force on Colorectal Cancer. *Official journal of the American College of Gastroenterology/ ACG* **115**, 415–434 (2020).
13. Liu, M. C. *et al.* Using New Hampshire Colonoscopy Registry data to assess United States and European post-polypectomy surveillance guidelines. *Endoscopy* **55**, 423–431 (2023).
14. Hagggar, F. A. & Boushey, R. P. Colorectal cancer epidemiology: incidence, mortality, survival, and risk factors. *Clinics in colon and rectal surgery* **22**, 191–7 (2009).
15. Wu, A. H., Paganini-Hill, A., Ross, R. K. & Henderson, B. E. Alcohol, physical activity and other risk factors for colorectal cancer: a prospective study. *British journal of cancer* **55**, 687–94 (1987).
16. Huxley, R. R. *et al.* The impact of dietary and lifestyle risk factors on risk of colorectal cancer: a quantitative overview of the epidemiological evidence. *International journal of cancer* **125**, 171–80 (2009).
17. Amersi, F., Agustin, M. & Ko, C. Y. Colorectal Cancer: Epidemiology, Risk Factors, and Health Services. *Clinics in Colon and Rectal Surgery* **18**, 133–140 (2005).

18. Friedenreich, C. M., Neilson, H. K. & Lynch, B. M. State of the epidemiological evidence on physical activity and cancer prevention. *European Journal of Cancer* **46**, 2593–2604 (2010).
19. Giovannucci, E. *et al.* Physical activity, obesity, and risk for colon cancer and adenoma in men. *Annals of internal medicine* **122**, 327–34 (1995).
20. Rafter, J. *et al.* Dietary synbiotics reduce cancer risk factors in polypectomized and colon cancer patients. *The American journal of clinical nutrition* **85**, 488–96 (2007).
21. Benito, E. *et al.* Nutritional factors in colorectal cancer risk: a case-control study in Majorca. *International journal of cancer* **49**, 161–7 (1991).
22. Fedirko, V. *et al.* Alcohol drinking and colorectal cancer risk: an overall and dose-response meta-analysis of published studies. *Annals of Oncology* **22**, 1958–1972 (2011).
23. Giovannucci, E. An updated review of the epidemiological evidence that cigarette smoking increases risk of colorectal cancer. *Cancer epidemiology, biomarkers & prevention : a publication of the American Association for Cancer Research, cosponsored by the American Society of Preventive Oncology* **10**, 725–31 (2001).
24. Rex, D. K., Alikhan, M., Cummings, O. & Ulbright, T. M. Accuracy of pathologic interpretation of colorectal polyps by general pathologists in community practice. *Gastrointestinal endoscopy* **50**, 468–74 (1999).
25. Terry, M. B. *et al.* Reliability in the classification of advanced colorectal adenomas. *Cancer epidemiology, biomarkers & prevention : a publication of the American Association for Cancer Research, cosponsored by the American Society of Preventive Oncology* **11**, 660–3 (2002).

26. Hetzel, J. T. *et al.* Variation in the Detection of Serrated Polyps in an Average Risk Colorectal Cancer Screening Cohort. *The American Journal of Gastroenterology* **105**, 2656–2664 (2010).
27. Jensen, P. *et al.* Observer variability in the assessment of type and dysplasia of colorectal adenomas, analyzed using kappa statistics. *Diseases of the colon and rectum* **38**, 195–8 (1995).
28. Yoon, H. *et al.* Inter-observer agreement on histological diagnosis of colorectal polyps: the APACC study. *Gastroenterologie clinique et biologique* **26**, 220–4 (2002).
29. Costantini, M. *et al.* Interobserver agreement in the histologic diagnosis of colorectal polyps. the experience of the multicenter adenoma colorectal study (SMAC). *Journal of clinical epidemiology* **56**, 209–14 (2003).
30. van Putten, P. G. *et al.* Inter-observer variation in the histological diagnosis of polyps in colorectal cancer screening. *Histopathology* **58**, 974–981 (2011).
31. Foss, F. A., Milkins, S. & McGregor, A. H. Inter-observer variability in the histological assessment of colorectal polyps detected through the NHS Bowel Cancer Screening Programme. *Histopathology* **61**, 47–52 (2012).
32. Mahajan, D. *et al.* Reproducibility of the Villous Component and High-grade Dysplasia in Colorectal Adenomas <1 cm. *The American Journal of Surgical Pathology* **37**, 427–433 (2013).
33. Lasisi, F. *et al.* Agreement in interpreting villous elements and dysplasia in adenomas less than one centimetre in size. *Digestive and Liver Disease* **45**, 1049–1055 (2013).

34. Osmond, A. *et al.* Interobserver variability in assessing dysplasia and architecture in colorectal adenomas: a multicentre Canadian study. *Journal of Clinical Pathology* **67**, 781–786 (2014).
35. Baldin, R. K. S. *et al.* Interobserver variability in histological diagnosis of serrated colorectal polyps. *Journal of Coloproctology* **35**, 193–197 (2015).
36. Anderson, J. C. *et al.* Clinically significant serrated polyp detection rates and risk for postcolonoscopy colorectal cancer: data from the New Hampshire Colonoscopy Registry. *Gastrointest Endosc* **96**, 310–317 (2022).
37. Anderson, J. C., Robinson, C. M. & Butterly, L. F. Increased risk of metachronous large serrated polyps in individuals with 5- to 9-mm proximal hyperplastic polyps: data from the New Hampshire Colonoscopy Registry. *Gastrointest Endosc* **92**, 387–393 (2020).
38. Anderson, J. C. *et al.* Risk of Metachronous High-risk Adenomas and Large Serrated Polyps in Individuals With Serrated Polyps on Index Colonoscopy: Data from the New Hampshire Colonoscopy Registry. *Gastroenterology* **154**, 117-127.e2 (2018).
39. Sirinukunwattana, K. *et al.* Locality sensitive deep learning for detection and classification of nuclei in routine colon cancer histology images. *IEEE transactions on medical imaging* **35**, 1196–1206 (2016).
40. Sornapudi, S. *et al.* Deep Learning Nuclei Detection in Digitized Histology Images by Superpixels. *Journal of Pathology Informatics* **9**, 5 (2018).
41. Chen, K., Zhang, N., Powers, L. & Roveda, J. Cell Nuclei Detection and Segmentation for Computational Pathology Using Deep Learning. in *2019 Spring Simulation Conference (SpringSim)* 1–6 (2019). doi:10.23919/SpringSim.2019.8732905.

42. Korbar, B. *et al.* Deep learning for classification of colorectal polyps on whole-slide images. *Journal of pathology informatics* **8**, 30 (2017).
43. Tomita, N. *et al.* Attention-Based Deep Neural Networks for Detection of Cancerous and Precancerous Esophagus Tissue on Histopathological Slides. *JAMA network open* **2**, e1914645 (2019).
44. Wei, J. W. *et al.* Automated detection of celiac disease on duodenal biopsy slides: A deep learning approach. *Journal of Pathology Informatics* **10**, (2019).
45. Nasir-Moin, M. *et al.* Evaluation of an Artificial Intelligence–Augmented Digital System for Histologic Classification of Colorectal Polyps. *JAMA Netw Open* **4**, e2135271 (2021).
46. Zhu, M. *et al.* Development and evaluation of a deep neural network for histologic classification of renal cell carcinoma on biopsy and surgical resection slides. *Scientific Reports* **11**, (2021).
47. Barrios, W. *et al.* Bladder cancer prognosis using deep neural networks and histopathology images. *J Pathol Inform* **13**, 100135 (2022).
48. Wei, J. W. *et al.* Evaluation of a Deep Neural Network for Automated Classification of Colorectal Polyps on Histopathologic Slides. *JAMA Network Open* **3**, 1–11 (2020).
49. Wu, W., Liu, X., Hamilton, R. B., Suriawinata, A. A. & Hassanpour, S. Graph Convolutional Neural Networks for Histologic Classification of Pancreatic Cancer. *Arch Pathol Lab Med* **147**, 1251–1260 (2023).
50. Yao, J., Zhu, X., Jonnagaddala, J., Hawkins, N. & Huang, J. Whole slide images based cancer survival prediction using attention guided deep multiple instance learning networks. *Medical Image Analysis* **65**, 101789–101789 (2020).

51. Jiang, S., Zanazzi, G. J. & Hassanpour, S. Predicting prognosis and IDH mutation status for patients with lower-grade gliomas using whole slide images. *Scientific Reports* **11**, 16849–16849 (2021).
52. Chen, R. J. *et al.* Multimodal Co-Attention Transformer for Survival Prediction in Gigapixel Whole Slide Images. 3995–4005 (2022) doi:10.1109/iccv48922.2021.00398.
53. Fan, L., Sowmya, A., Meijering, E. & Song, Y. Cancer Survival Prediction From Whole Slide Images With Self-Supervised Learning and Slide Consistency. *IEEE Transactions on Medical Imaging* **42**, 1401–1412 (2023).
54. Zidan, U., Gaber, M. M. & Abdelsamea, M. M. SwinCup: Cascaded swin transformer for histopathological structures segmentation in colorectal cancer. *Expert Systems with Applications* **216**, 119452 (2023).
55. Cai, H. *et al.* MIST: multiple instance learning network based on Swin Transformer for whole slide image classification of colorectal adenomas. *The Journal of pathology* (2022) doi:10.1002/PATH.6027.
56. Wagner, S. J. *et al.* Fully transformer-based biomarker prediction from colorectal cancer histology: a large-scale multicentric study. *arXiv preprint arXiv:2301.09617* (2023).
57. Boehm, K. M., Khosravi, P., Vanguri, R., Gao, J. & Shah, S. P. Harnessing multimodal data integration to advance precision oncology. *Nature Reviews Cancer* **22**, 114–126 (2022).
58. Mobadersany, P. *et al.* Predicting cancer outcomes from histology and genomics using convolutional networks. (2018) doi:10.1073/pnas.1717139115.
59. Jiang, S., Zanazzi, G. J. & Hassanpour, S. Predicting prognosis and IDH mutation status for patients with lower-grade gliomas using whole slide images. *Sci Rep* **11**, 16849 (2021).

60. Lu, M. Y. *et al.* Data-efficient and weakly supervised computational pathology on whole-slide images. *Nature Biomedical Engineering* **5**, 555–570 (2021).
61. Yan, R. *et al.* Richer fusion network for breast cancer classification based on multimodal data. *BMC Medical Informatics and Decision Making* **21**, 1–15 (2021).
62. Cheerla, A. & Gevaert, O. Deep learning with multimodal representation for pancancer prognosis prediction. in vol. 35 i446–i454 (2019).
63. Wang, H., Subramanian, V. & Syeda-Mahmood, T. Modeling uncertainty in multi-modal fusion for lung cancer survival analysis. in *2021 IEEE 18th international symposium on biomedical imaging (ISBI)* 1169–1172 (IEEE, 2021).
64. Huang, J., Tao, J., Liu, B., Lian, Z. & Niu, M. Multimodal Transformer Fusion for Continuous Emotion Recognition. in 3507–3511 (2020). doi:10.1109/ICASSP40776.2020.9053762.
65. Greene, M. A. *et al.* Matching colonoscopy and pathology data in population-based registries: development of a novel algorithm and the initial experience of the New Hampshire Colonoscopy Registry. *Gastrointestinal endoscopy* **74**, 334–40 (2011).
66. Yim, M., Butterly, L. F., Goodrich, M. E., Weiss, J. E. & Onega, T. L. Perception of colonoscopy benefits: a gap in patient knowledge? *Journal of community health* **37**, 719–24 (2012).
67. Jiang, S., Hondelink, L., Suriawinata, A. A. & Hassanpour, S. Masked pre-training of transformers for histology image analysis. *Journal of Pathology Informatics* 100386 (2024) doi:10.1016/j.jpi.2024.100386.
68. Carney, P., Goodrich, M., Butterly, L. & Dietrich, A. The design and development of a population-based colonoscopy registry. *J Regis Manag* **33**, 91–99 (2006).

69. Butterly, L., Olenec, C., Goodrich, M., Carney, P. & Dietrich, A. Colonoscopy Demand and Capacity in New Hampshire. *American Journal of Preventive Medicine* **32**, 25–31 (2007).
70. Strum, W. B. Colorectal Adenomas. *New England Journal of Medicine* **374**, 1065–1075 (2016).
71. Muto, T., Bussey, H. J. & Morson, B. C. The evolution of cancer of the colon and rectum. *Cancer* **36**, 2251–70 (1975).
72. Otchy, D. P. *et al.* Metachronous colon cancer in persons who have had a large adenomatous polyp. *The American journal of gastroenterology* **91**, 448–54 (1996).
73. Atkin, W. S., Morson, B. C. & Cuzick, J. Long-Term Risk of Colorectal Cancer after Excision of Rectosigmoid Adenomas. *New England Journal of Medicine* **326**, 658–662 (1992).
74. Imperiale, T. F. *et al.* Risk of Advanced Proximal Neoplasms in Asymptomatic Adults According to the Distal Colorectal Findings. *New England Journal of Medicine* **343**, 169–174 (2000).
75. O’Connell, B. M. & Crockett, S. D. The clinical impact of serrated colorectal polyps. *Clinical epidemiology* **9**, 113–125 (2017).
76. He, K., Zhang, X., Ren, S. & Sun, J. Delving deep into rectifiers: Surpassing human-level performance on imagenet classification. in *Proceedings of the IEEE International Conference on Computer Vision* 1026–1034 (2015).
77. Jiang, S., Suriawinata, A. A. & Hassanpour, S. MHAttnSurv: Multi-head attention for survival prediction using whole-slide pathology images. *Computers in Biology and Medicine* 106883 (2023) doi:<https://doi.org/10.1016/j.compbiomed.2023.106883>.

78. Wang, W., Tran, D. & Feiszli, M. What makes training multi-modal classification networks hard? in *Proceedings of the IEEE/CVF conference on computer vision and pattern recognition* 12695–12705 (2020).

Supplementary Table 1. Extracted data from NHCR for patients undergoing colorectal polyp biopsy organized in four categories.

Category	Extracted Data
Personal history	Age, gender, race and ethnicity, marital status
	Height, weight, body mass index
	Smoking status (duration, cigarettes per day)
	Alcohol consumption (drinks per week)
	Exercise routine, activity level
	Vitamin supplement use (quantity)
	Calcium supplement use (quantity)
Medical history	Familial adenomatous polyposis
	Hereditary non-polyposis CRC
	Crohn's disease or ulcerative colitis
	Constipation or colorectal bleeding
	Aspirin use (dosage)
Family history	Relatives diagnosed with CRC (mother/father/sister/brother/child)
	Age of relatives at diagnosis (<50, 50-60, >60)
	Relatives diagnosed with colorectal polyps, familial adenomatous polyposis, hereditary non-polyposis CRC, familial polyposis
Endoscopy history	Preparation type
	Last sigmoidoscopy and colonoscopy time
	Last sigmoidoscopy and colonoscopy outcome

Supplementary Table 1. Demographical features of the study population

Variable	Level	Missing	Grouped by risk		P-Value
			Low Risk	High Risk	
n			1994	399	
Age, mean (SD)		0	58.7 (9.8)	62.0 (8.5)	<0.001
Gender, n (%)	F	0	959 (48.1)	157 (39.3)	0.002
	M		1035 (51.9)	242 (60.7)	
Hispanic, n (%)	Hispanic	456	18 (1.1)	4 (1.2)	0.778
	Not Hispanic		1593 (98.9)	322 (98.8)	
Race, n (%)	African American	454	5 (0.3)		0.509
	American Indian		3 (0.2)		
	Asian		6 (0.4)	2 (0.6)	
	Caucasian		1548 (95.9)	314 (96.6)	
	Multiple		41 (2.5)	9 (2.8)	
	Other		11 (0.7)		

Supplementary Table 3. Patient description: Personal history

Variable	Level	Missing	Grouped by risk		P-Value
			Low Risk	High Risk	
n			1994	399	
Age, mean (SD)		0	58.7 (9.8)	62.0 (8.5)	<0.001
Gender, n (%)	F	0	959 (48.1)	157 (39.3)	0.002
	M		1035 (51.9)	242 (60.7)	
Marital Status, n (%)	Single	494	113 (7.2)	20 (6.2)	0.451
	Married		1196 (75.8)	241 (75.1)	
	Separated		14 (0.9)	4 (1.2)	
	Divorced		158 (10.0)	31 (9.7)	
	Widowed		53 (3.4)	18 (5.6)	
	Living as married		44 (2.8)	7 (2.2)	
Hispanic, n (%)	Hispanic	456	18 (1.1)	4 (1.2)	0.778
	Not Hispanic		1593 (98.9)	322 (98.8)	
Race, n (%)	African American	454	5 (0.3)		0.509
	American Indian		3 (0.2)		
	Asian		6 (0.4)	2 (0.6)	
	Caucasian		1548 (95.9)	314 (96.6)	
	Multiple		41 (2.5)	9 (2.8)	
	Other		11 (0.7)		
Exercise, n (%)	No exercise	466	136 (8.5)	37 (11.4)	0.029
	Active daily life		549 (34.2)	128 (39.5)	
	1-5 times/week		760 (47.4)	126 (38.9)	
	5+ times/week		158 (9.9)	33 (10.2)	
Smoker status, n (%)	Never smoker	453	744 (46.2)	148 (45.1)	0.905
	Former smoker		694 (43.1)	141 (43.0)	
	Current smoker		167 (10.4)	38 (11.6)	
	Error		7 (0.4)	1 (0.3)	
Qty smoke, n (%)	Nonsmoker	506	744 (47.5)	148 (46.1)	0.949
	10 or fewer cigarettes/day		262 (16.7)	54 (16.8)	
	11-20/day		345 (22.0)	71 (22.1)	
	21-30/day		152 (9.7)	32 (10.0)	
	31+/day		63 (4.0)	16 (5.0)	
Years of smoking, mean (SD)		498	10.3 (13.2)	11.7 (14.8)	0.123
Weekly alcohol intake, n (%)	0 alcoholic drinks/week	471	586 (36.7)	116 (35.6)	0.423
	1-4 alcoholic drinks/week		504 (31.6)	101 (31.0)	
	5-8 alcoholic drinks/week		250 (15.7)	51 (15.6)	
	9-20 alcoholic drinks/week		232 (14.5)	48 (14.7)	
	21+ alcoholic drinks/week		24 (1.5)	10 (3.1)	
Calcium, n (%)	No calcium use	1854	292 (61.5)	43 (67.2)	0.455
	Calcium use		183 (38.5)	21 (32.8)	
Vitamins, n (%)	No vitamin use	1012	383 (34.2)	76 (29.2)	0.147
	Vitamin use		738 (65.8)	184 (70.8)	
Patient weight in inches, mean (SD)		462	183.1 (42.4)	191.2 (43.2)	0.002
Patient height in pounds, mean (SD)		459	67.2 (4.2)	67.8 (4.5)	0.015
BMI, median [Q1, Q3]		482	27.0 [24.0,31.0]	28.0 [25.0,32.0]	0.014

Supplementary Table 4. Patient description: Medical history

Variable	Level	Missing	Grouped by risk		P-Value
			Low risk	High risk	
n			1994	399	
History of IBD, n (%)	No	152	1764 (94.3)	357 (96.5)	0.111
	Yes		107 (5.7)	13 (3.5)	
Genetic syndrome, n (%)	No	336	1711 (99.9)	344 (100.0)	1.000
	Yes		2 (0.1)		
Diag exam-change in bowel habits, n (%)	No	351	1691 (99.1)	335 (99.7)	0.495
	Yes		15 (0.9)	1 (0.3)	
Diag exam-Evaluate GI bleeding, n (%)	No	351	1659 (97.2)	325 (96.7)	0.731
	Yes		47 (2.8)	11 (3.3)	
Aspirin use, n (%)	No	527	896 (57.5)	150 (48.5)	0.004
	Yes		661 (42.5)	159 (51.5)	

Supplementary Table 5. Patient description: Family history

Variable	Level	Missing	Grouped by risk		P-Value
			Low risk	High risk	
n			1994	399	
Screening exam for family hx of polyp(s), n (%)	No	351	1584 (92.8)	315 (93.8)	0.635
	Yes		122 (7.2)	21 (6.2)	
Has a biological family member ever had colon polyps, n (%)	No	447	366 (22.6)	59 (18.0)	0.129
	Yes		522 (32.3)	105 (32.0)	
	Don't know		730 (45.1)	164 (50.0)	
Has a family history of CRC in a first-degree relative, n (%)	No	417	1196 (73.5)	253 (72.7)	0.822
	Yes		432 (26.5)	95 (27.3)	
Has a family history of CRC in first-degree relative under 50, n (%)	No	641	1369 (94.3)	279 (93.0)	0.470
	Yes		83 (5.7)	21 (7.0)	
Has a family history of CRC in first-degree relative under 60, n (%)	No	660	1276 (89.4)	264 (86.6)	0.190
	Yes		152 (10.6)	41 (13.4)	
Patient family member has genetic syndrome, n (%)	No	344	1684 (98.7)	338 (98.5)	0.795
	Yes		22 (1.3)	5 (1.5)	

Supplementary Table 6. Patient description: Endoscopy history

Variable	Level	Missing	Grouped by risk		P-Value
			Low risk	High risk	
n			1994	399	
Procedure - exam preparation quality, n (%)	Excellent	565	486 (31.7)	74 (25.1)	0.006
	Good		906 (59.1)	203 (68.8)	
	Fair		141 (9.2)	18 (6.1)	
Type of preparation: Nulytely, n (%)	No	104	1567 (81.8)	341 (91.2)	<0.001
	Yes		348 (18.2)	33 (8.8)	
Type of preparation: Osmoprep (pills), n (%)	No	104	1915 (100.0)	374 (100.0)	1.000
Type of preparation: Half Lytely, n (%)	No	104	1866 (97.4)	368 (98.4)	0.359
	Yes		49 (2.6)	6 (1.6)	
Type of preparation: Fleet, n (%)	No	104	1909 (99.7)	373 (99.7)	1.000
	Yes		6 (0.3)	1 (0.3)	
Type of preparation: Other, n (%)	No	104	1907 (99.6)	372 (99.5)	0.672
	Yes		8 (0.4)	2 (0.5)	
Last sigmoid/colonoscopy Pilot only, n (%)	Never	1835	141 (28.7)	17 (25.8)	0.533
	Within last 12 months		12 (2.4)	4 (6.1)	
	1-4 years ago		114 (23.2)	17 (25.8)	
	5-10 years ago		202 (41.1)	25 (37.9)	
	More than 10 years ago		23 (4.7)	3 (4.5)	
Time since last colonoscopy, n (%)	Never	982	381 (33.1)	76 (29.2)	0.254
	Within last 12 months		39 (3.4)	10 (3.8)	
	1-4 years ago		211 (18.2)	44 (16.9)	
	5-10 years ago		464 (40.3)	108 (41.5)	
	More than 10 years ago		56 (4.9)	22 (8.5)	
Previous colonoscopy findings: polyps, n (%)	No	979	760 (65.9)	155 (59.4)	0.055
	Yes		393 (34.1)	106 (40.6)	
Previous colonoscopy findings: diverticulosis, n (%)	No	979	1087 (94.3)	248 (95.0)	0.747
	Yes		66 (5.7)	13 (5.0)	
Previous colonoscopy findings: hemorrhoids, n (%)	No	979	1081 (93.8)	241 (92.3)	0.484
	Yes		72 (6.2)	20 (7.7)	
Previous colonoscopy findings: other, n (%)	No	979	1108 (96.1)	253 (96.9)	0.643
	Yes		45 (3.9)	8 (3.1)	
Previous colonoscopy findings: no findings, n (%)	No	979	842 (73.0)	193 (73.9)	0.822
	Yes		311 (27.0)	68 (26.1)	
Previous colonoscopy results: do not know, n (%)	No	1872	386 (96.0)	115 (96.6)	1.000
	Yes		16 (4.0)	4 (3.4)	

Supplementary Table 7. Patient description: Current colonoscopy exam

Variable	Level	Missing	Grouped by risk		P-Value
			Low risk	High risk	
n			1994	399	
Number of records where an adenoma was indicated, median [Q1, Q3]		0	1.0 [0.0,1.0]	1.0 [1.0,3.0]	<0.001
Largest known adenoma size, n (%)	No adenoma	148	599 (31.8)	70 (19.2)	<0.001
	<5mm		788 (41.9)	142 (39.0)	
	5-9mm		333 (17.7)	96 (26.4)	
	10-20mm		132 (7.0)	50 (13.7)	
	>20mm		29 (1.5)	6 (1.6)	
Any advanced adenoma at the procedure level, n (%)	No	186	1657 (89.3)	273 (77.8)	<0.001
	Yes		199 (10.7)	78 (22.2)	
Any adenoma at the procedure level, n (%)	No	0	599 (30.0)	70 (17.5)	<0.001
	Yes		1395 (70.0)	329 (82.5)	
Any HP at the procedure level, n (%)	No	0	1182 (59.3)	274 (68.7)	0.001
	Yes		812 (40.7)	125 (31.3)	
Any SSA/P or TSA w/wo dysplasia at the procedure level, n (%)	No	0	1784 (89.5)	342 (85.7)	0.037
	Yes		210 (10.5)	57 (14.3)	
Any CSSP at the procedure level, n (%)	No	164	1569 (84.9)	306 (80.5)	0.043
	Yes		280 (15.1)	74 (19.5)	
Number of serrated lesions identified, median [Q1, Q3]		0	0.0 [0.0,1.0]	0.0 [0.0,1.0]	0.083
Largest known serrated (missing path/size ignored), n (%)	No serrated polyp	140	1036 (55.3)	238 (62.5)	<0.001
	<5mm		585 (31.2)	75 (19.7)	
	5-9mm		171 (9.1)	48 (12.6)	
	10-20mm		71 (3.8)	17 (4.5)	
	>20mm		9 (0.5)	3 (0.8)	

Supplementary Table 8. Patient description: Pathologist assessments

Variable	Level	Missing	Grouped by risk		P-Value
			Low risk	High risk	
n			1994	399	
Most advanced adenoma at tissue level, n (%)	No adenoma	0	781 (39.2)	119 (29.8)	0.002
	Tubular adenoma		1159 (58.1)	263 (65.9)	
	Tubulovillous adenoma		48 (2.4)	14 (3.5)	
	Villous adenoma		6 (0.3)	3 (0.8)	
Most advanced serrated at tissue level, n (%)	No serrated polyp	0	1353 (67.9)	299 (74.9)	0.001
	Hyperplastic polyp		489 (24.5)	61 (15.3)	
	SSP without dysplasia		129 (6.5)	35 (8.8)	
	SSP with dysplasia		15 (0.8)	2 (0.5)	
	TSA		8 (0.4)	2 (0.5)	

Supplementary Table 9. Feature importance calculated from permutation

Variable	Importance
Number of adenomas	0.029 (0.010)
WSI risk score	0.016 (0.009)
Age	0.016 (0.002)
Nulytely preparation	0.011 (0.004)
Any CSSP	0.006 (0.002)
Number of serrated lesions	0.005 (0.003)
Any SSA/P or TSA w/wo dysplasia	0.004 (0.001)
Any advanced adenoma	0.003 (0.002)
Vitamins	0.003 (0.002)
Family member ever had colon polyps	0.002 (0.001)